IOSR Journal of Applied Physics (IOSR-JAP)
e-ISSN: 2278-4861.Volume 18, Issue 2 Ser. II (Mar – Apr 2026), PP 16-23
www.iosrjournals.org

Spectral, Thermal and Luminescent Properties of Nd^{3+} Doped Borophosphate Glasses for 1075 nm NIR Photonic broad band Amplification applications

S.L.Meena
Ceramic Laboratory, Department of physics, Jai Narain Vyas University, Jodhpur 342001(Raj.) India

Abstract
Glass of the system :(30-x)P_2O_5:10ZnO:10Li_2O:10Na_2O:10CaO:10WO_3:20B_2O_3:xNd_2O_3, (where x=1, 1.5,2 mol %) have been prepared by melt-quenching method. The amorphous nature of the glasses was confirmed by X-ray diffraction studies. DTA curve was analysed to evaluate the glass transition temperature, crystallization temperature and melting temperature and hence study the thermal properties. Optical absorption spectra were recorded at room temperature for all glass samples. Slater-Condon parameters F_k (k=2, 4, 6), Lande parameter ξ_{4f} and Racah parameters E^k (k=1, 2, 3) have been computed. Using these parameters energies and intensities of these bands has been calculated. Judd-Ofelt intensity parameters Ω_λ (λ=2, 4, 6) are evaluated from the intensities of various absorption bands of optical absorption spectra. Using these intensity parameters various radiative properties like spontaneous emission probability (A), branching ratio (β_R), radiative life time (τ_R) and stimulated emission cross–section (σ_p)) of various emission lines have been evaluated.

Keywords: *ZLSLTBP Glasses, Thermal Properties, Judd-Ofelt Theory, Photoluminescence Properties.*

I. Introduction

Glasses with different compositions very attractive material to investigate various properties such as high refractive index, large third order nonlinear optical susceptibility, high density, low melting temperature and excellent transparency[1-5].Phosphate glass is an extremely promising material for sensors, reflecting windows, fiber optics ,optical amplifier and nonlinear applications in optics due to some of its essential characteristic features, such as low melting temperature ,low phonon energy and high thermal stability [6-8].Phosphate glasses have excellent transparency, good thermal and mechanical stability. They present superior properties like that high transparency, high density, low melting point and high solubility for rare-earth ions. Due to their good chemical durability,Nd^{3+} doped phosphate glasses are attractive materials for the fabrication of low cost integrated optical amplifiers by using the ion exchange technique. The addition of network modifier (NWF) Li_2O is to improve both mechanical and electrical properties of such glasses. Zinc oxide is added in the glass matrix to increase glass forming ability and to ensure low rates of crystallization in the glass system. Among active rare-earth ions Nd^{3+} exhibits high solubility in ceramic glasses, which also possess excellent physical, optical and thermal, properties [9-13].

The present work reports on the absorption, thermal and luminescent properties of Nd^{3+} doped zinc lithium sodalime tungsten borophosphate glass. The intensities of the transitions for the rare earth ions have been estimated successfully using the Judd-Ofelt theory, The laser parameters such as radiative probabilities (A), branching ratio (β_R), radiative life time (τ_R) and stimulated emission cross section(σ_p) are evaluated using J.O. intensity parameters (Ω_λ, λ=2,4 and 6).

II. Experimental Techniques

Preparation of glasses

The following Nd^{3+} doped borophosphate glass samples :(30-x)P_2O_5:10ZnO:10Li_2O:10Na_2O:10CaO:10WO_3:20B_2O_3:xNd_2O_3.(where x =1, 1.5, 2) have been prepared by melt-quenching method. Analytical reagent grade chemical used in the present study consist of P_2O_5, ZnO, Li_2O, Na_2O, CaO,WO_3, B_2O_3 and Nd_2O_3. They were thoroughly mixed by using an agate pestle mortar. Then melted at 975˚C by an electrical muffle furnace for 2 hours. After complete melting, the melts were quickly poured in to a preheated stainless steel mould and annealed at temperature of 250˚C for 2 h to remove thermal strains and stresses. Every time fine powder of cerium oxide was used for polishing the samples. The glass samples so prepared were of good optical quality and were transparent. The chemical compositions of the glasses with the name of samples are summarized in **Table 1.**

Table 1.

Sample	Glass composition (mol %)
ZLSLTBP (UD)	$30P_2O_5$:10ZnO:$10Li_2O$:$10Na_2O$:10CaO:$10WO_3$:$20B_2O_3$
ZLSLTBP ND(1.0)	$29P_2O_5$:10ZnO:$10Li_2O$:$10Na_2O$:10CaO:$10WO_3$:$20B_2O_3$:$1Nd_2O_3$
ZLSLTBP ND(1.5)	$28.5P_2O_5$:10ZnO:$10Li_2O$:$10Na_2O$:10CaO:$10WO_3$:$20B_2O_3$:$1.5Nd_2O_3$
ZLSLTBP ND(2.0)	$28P_2O_5$:10ZnO:$10Li_2O$:$10Na_2O$:10CaO:$10WO_3$:$20B_2O_3$: $2Nd_2O_3$

ZLSLTBP (UD) - Represents undoped Zinc Lithium Sodalime Tungsten Borophosphate glass specimen.
ZLSLTBP (ND) - Represents Nd^{3+} doped Zinc Lithium Sodalime Tungsten Borophosphate glass specimens.

III. Theory

3.1 Oscillator Strength

The intensity of spectral lines is expressed in terms of oscillator strengths using the relation [14].

$$f_{expt.} = 4.318 \times 10^{-9} \int \varepsilon(\nu)\, d\nu \qquad (1)$$

where, $\varepsilon(\nu)$ is molar absorption coefficient at a given energy ν (cm^{-1}), to be evaluated from Beer–Lambert law. Under Gaussian Approximation, using Beer–Lambert law, the observed oscillator strengths of the absorption bands have been experimentally calculated [15], using the modified relation:

$$P_m = 4.6 \times 10^{-9} \times \frac{1}{cl} \log \frac{I_0}{I} \times \Delta\upsilon_{1/2} \qquad (2)$$

Where c is the molar concentration of the absorbing ion per unit volume, I is the optical path length, $\log I_0/I$ is optical density and $\Delta\upsilon_{1/2}$ is half band width.

3.2. Judd-Ofelt Intensity Parameters

According to Judd [16] and Ofelt [17] theory, independently derived expression for the oscillator strength of the induced forced electric dipole transitions between an initial J manifold $|4f^N (S, L) J\rangle$ level and the terminal J' manifold $|4f^N (S', L') J'\rangle$ is given by:

$$\frac{8\Pi^2 mc\bar{\upsilon}}{3h(2J+1)} \frac{1}{n} \left[\frac{(n^2+2)^2}{9}\right] \times S(J, J') \qquad (3)$$

Where, the line strength S (J, J') is given by the equation

$$S(J, J') = e^2 \sum_{\lambda = 2, 4, 6} \Omega_\lambda \langle 4f^N (S, L) J \| U^{(\lambda)} \| 4f^N (S', L') J' \rangle^2 \qquad (4)$$

In the above equation m is the mass of an electron, c is the velocity of light, ν is the wave number of the transition, h is Planck's constant, n is the refractive index, J and J' are the total angular momentum of the initial and final level respectively, Ω_λ (λ=2,4and 6) are known as Judd-Ofelt intensity parameters.

3.3 Radiative Properties

The Ω_λ parameters obtained using the absorption spectral results have been used to predict radiative properties such as spontaneous emission probability (A) and radiative life time (τ_R), and laser parameters like fluorescence branching ratio (β_R) and stimulated emission cross section (σ_p).

The spontaneous emission probability from initial manifold $|4f^N (S', L') J'\rangle$ to a final manifold $|4f^N (S, L) J\rangle$ is given by:

$$A[(S', L') J'; (S, L) J] = \frac{64\pi^2 \nu^3}{3h(2J'+1)} \left[\frac{n(n^2+2)^2}{9}\right] \times S(J', J) \qquad (5)$$

Where, $S(J', J) = e^2 [\Omega_2 \| U^{(2)} \|^2 + \Omega_4 \| U^{(4)} \|^2 + \Omega_6 \| U^{(6)} \|^2]$

The fluorescence branching ratio for the transitions originating from a specific initial manifold $|4f^N (S', L') J'>$ to a final many fold $|4f^N (S, L) J >$ is given by

$$\beta [(S', L') J'; (S, L) J] = \sum_{S L J} \frac{A[(S' L)]}{A[(S' L') J' (\bar{S} L)]} \quad (6)$$

The radiative life time is given by

$$\tau_{rad} = \sum_{S L J} A[(S', L') J'; (S, L)] = A^{-1}_{Total} \quad (7)$$

Where, the sum is over all possible terminal manifolds. The stimulated emission cross -section for a transition from an initial manifold $|4f^N (S', L') J'>$ to a final manifold $|4f^N (S, L) J >|$ is expressed as

$$\sigma_p(\lambda_p) = \left[\frac{\lambda_p^4}{8\pi c n^2 \Delta\lambda_{eff}}\right] \times A[(S', L') J'; (\bar{S}, \bar{L}) \bar{J}] \quad (8)$$

Where, λ_p the peak fluorescence wavelength of the emission band and $\Delta\lambda_{eff}$ is the effective fluorescence line width.

3.4 Nephelauxetic Ratio (β) and Bonding Parameter ($b^{1/2}$)

The nature of the R-O bond is known by the Nephelauxetic Ratio (β') and Bonding Parameters ($b^{1/2}$), which are computed by using following formulae [18,19]. The Nephelauxetic Ratio is given by

$$\beta' = \frac{\nu_g}{\nu_a} \quad (9)$$

where, ν_a and ν_g refer to the energies of the corresponding transition in the glass and free ion, respectively. The values of bonding parameter $b^{1/2}$ are given by

$$b^{1/2} = \left[\frac{1-\beta'}{2}\right]^{1/2} \quad (10)$$

IV. Result and Discussion

4.1. XRD Measurement

Figure 1 presents the XRD pattern of the samples shows no sharp Bragg's peak, but only a broad diffuse hump around low angle region. This is the clear indication of amorphous nature within the resolution limit of XRD instrument.

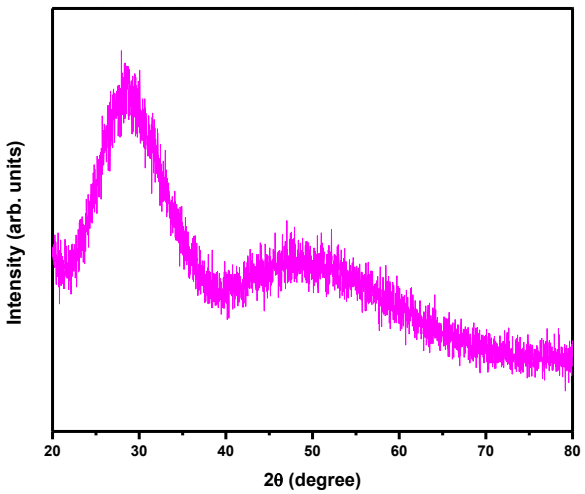

Fig.1: X-ray diffraction pattern of ZLSLTBP ND (1.0) glass.

4.3 Thermal Property

Differential thermal analysis checks the heat absorbed by glass samples during heating or cooling. Fig. 2 depicts the DTA thermogram of powdered ZLSLTBP sample. The glass transition temperature (T_g), onset crystallization temperature (T_c), crystallization temperature (T_p), melting temperature(T_m), thermal stability (T_s),Balaji Parameter (B_P), Hurbe's criterion (H_R) and reduced glass transition temperature (T_{rg}) were calculated. Shankar's parameter also calculated by using eq. (15). All the determined thermal parameters are given in table 2.

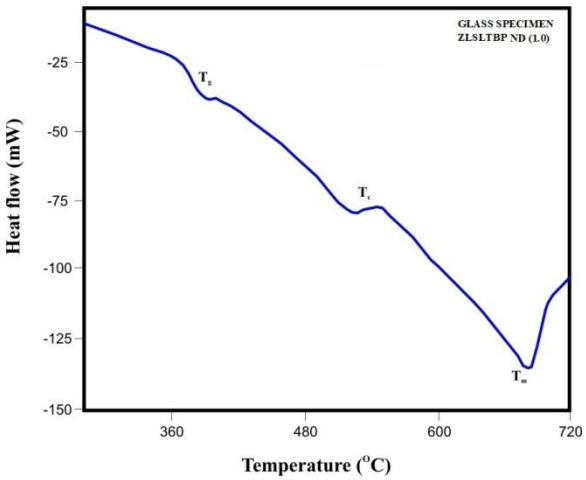

Fig.2: DTA curve of ZLSLTBP ND (1.0) glass.

Table 2. Thermal parameters determined from the DTA traces of ZLSLTBP ND glasses.

Sample Name	T_g (^{0}C)	T_c(^{0}C)	T_p(^{0}C)	T_m(^{0}C)	T_s(^{0}C)	B_P(^{0}C)	H_R(^{0}C)	K_S(^{0}C)	T_{rg}(^{0}C)
ZLSLTBP ND (1.0)	377	508	548	685	131	3.275	0.226	33.85	0.550
ZLSLTBP ND (1.5)	381	510	550	688	129	3.225	0.225	33.38	0.554
ZLSLTBP ND (2.0)	384	512	555	692	128	2.977	0.239	33.29	0.555

The thermal stability of the glass samples can be calculated by difference between onset crystallization temperature and transition temperature [20].

Thermal stability (T_s) =T_c-T_g (11)

Balaji Parameter can be calculated using [20].

Balaji Parameter (B_P) = $[(T_c-T_g)/(T_p-T_c)]$ (12)

Hruby's criterion is calculated using the Hurby's relation [20].

Hruby's criterion (H_R) = $[(T_p-T_c)/(T_m-T_c)]$ (13)

Reduced glass transition temperature is given as [20].

Reduced glass transition temperature (T_{rg}) =T_g/T_m (14)

Thermal Parameter is given as [20].

$K_S= [(T_m-T_c)\ (T_c-T_g)/T_m]$ (15)

4.2. Absorption spectra

The absorption spectra of ZLSLTBP ND(1.0) glass, consists of absorption bands corresponding to the absorptions from the ground state $^4I_{9/2}$ of Nd^{3+} ions. Nine absorption bands have been observed from the ground state $^4I_{9/2}$ to excited states $^4F_{3/2}$, $^4F_{5/2}$, $^4F_{7/2}$, $^4F_{9/2}$, $^2H_{11/2}$, $^4G_{5/2}$, $^4G_{7/2}$, $^4G_{9/2}$, and $^2G_{9/2}$ for Nd^{3+} doped ZLSLTBP ND(1.0) glass.

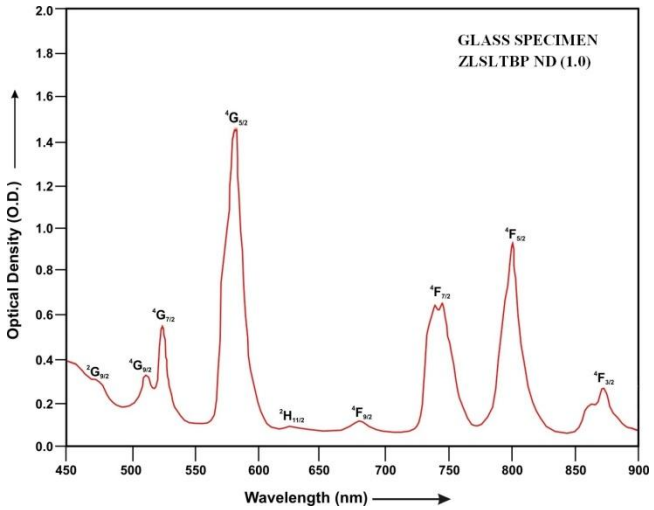

Fig.3: Absorption spectra of ZLSLTBP ND (1.0) glass.

The experimental and calculated oscillator strength for Nd^{3+} ions in ZLSLTBP glasses are given in **Table 3.**

Table 3. Measured and calculated oscillator strength ($P^m \times 10^{+6}$) of Nd^{3+} ions in ZLSLTBP glasses.

Energy level from $^4I_{9/2}$	Glass ZLSLTBP ND(1.0)		Glass ZLSLTBP ND(1.5)		Glass ZLSLTBP ND(2.0)	
	$P_{exp.}$	$P_{cal.}$	$P_{exp.}$	$P_{cal.}$	$P_{exp.}$	$P_{cal.}$
$^4F_{3/2}$	4.25	4.19	4.21	4.18	4.17	4.17
$^4F_{5/2}$	9.45	9.25	9.40	9.20	9.34	9.16
$^4F_{7/2}$	9.88	10.20	9.83	10.17	9.78	10.13
$^4F_{9/2}$	0.85	0.56	0.83	0.56	0.80	0.55
$^2H_{11/2}$	0.48	0.16	0.45	0.16	0.41	0.16
$^4G_{5/2}$	25.85	26.02	24.76	24.94	23.65	23.86
$^4G_{7/2}$	4.95	5.68	4.91	5.60	4.86	5.51
$^4G_{9/2}$	2.96	2.53	2.93	2.52	2.89	2.50
$^2G_{9/2}$	0.97	3.27	0.95	3.26	0.92	3.25
r.m.s.deviation	0.8422		0.8391		0.8397	

Table4. Computed values of Slater-Condon, Lande, Racah, nephelauexetic ratio and bonding parameter for Nd^{3+} doped ZLSLTBP glass specimens.

Parameter	Free ion	ZLSLTBP ND (1.0)	ZLSLTBP ND (1.5)	ZLSLTBP ND (2.0)
$F_2(cm^{-1})$	331.16	324.64	324.64	324.64
$F_4(cm^{-1})$	50.71	50.71	50.72	50.72
$F_6(cm^{-1})$	5.154	5.041	5.041	5.041
$\xi_{4f}(cm^{-1})$	884.0	882.67	882.67	882.67
$E^1(cm^{-1})$	5024.0	4948.19	4948.19	494.82
$E^2(cm^{-1})$	23.90	23.09	23.09	23.09
$E^3(cm^{-1})$	497.0	489.58	489.58	489.58
F_4/F_2	0.1531	0.1562	0.1562	0.1562
F_6/F_2	0.0155	0.0155	0.0155	0.0155
E^1/E^3	10.1086	10.1070	10.1070	10.1070
E^2/E^3	0.0481	0.0472	0.0472	0.0472
β'		0.9960	0.9960	0.9960
$b^{1/2}$		0.04449	0.04449	0.04449

The values of Judd-Ofelt intensity parameters are given in **Table 5**.

Table 5. Judd-Ofelt intensity parameters for Nd^{3+} doped ZLSLTBP glass specimens.

Glass Specimen	$\Omega_2(pm^2)$	$\Omega_4(pm^2)$	$\Omega_6(pm^2)$	Ω_4/Ω_6	Ref.
ZLSLTBP ND (1.0)	1.743	8.847	3.550	2.492	P.W.
ZLSLTBP ND (1.5)	1.402	8.816	3.534	2.495	P.W.
ZLSLTBP ND (2.0)	1.056	8.788	3.521	2.496	P.W.
PKABP (ND)	3.086	6.263	5.417	1.156	[21]

TN (ND)	4.060	4.790	4.620	1.037	[22]
Germanate	3.450	4.020	3.660	1.098	[23]
Zinc Tellurite	3.800	4.940	4.540	1.088	[24]
TeNd25	4.210	5.970	5.450	1.095	[25]

4.3. Excitation Spectrum

The Excitation spectra of Nd^{3+}doped ZLSLTBP ND (1.0) glass specimen has been presented in Figure 4 in terms of Excitation Intensity versus wavelength. The excitation spectrum was recorded in the spectral region 700–1000 nm fluorescence at 1065nm having different excitation band centred at 808 nm and 887 nm are attributed to the ($^4I_{9/2}\rightarrow{}^4F_{5/2}$) and ($^4I_{9/2}\rightarrow{}^4F_{3/2}$) transitions, respectively. The highest absorption level is ($^4I_{9/2}\rightarrow{}^4F_{5/2}$) and is at 808 nm. So this is to be chosen for excitation wavelength.

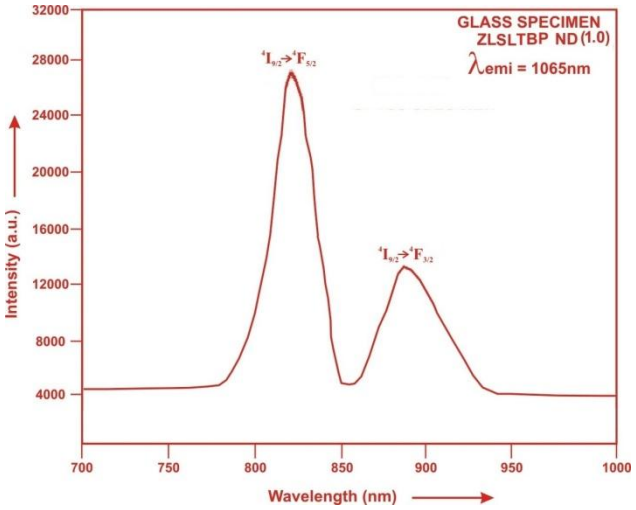

Fig.4: Excitation spectra of ZLSLTBP ND (1.0) glass.

4.4. Fluorescence Spectrum

The fluorescence spectrum of Nd^{3+}doped in zinc lithium sodalime tungsten borophosphate is shown in Figure 5. There are six broad bands ($^4G_{7/2}\rightarrow{}^4I_{9/2}$), ($^4G_{7/2}\rightarrow{}^4I_{11/2}$), ($^4F_{3/2}\rightarrow{}^4I_{9/2}$) ($^4F_{3/2}\rightarrow{}^4I_{11/2}$), ($^4F_{3/2}\rightarrow{}^4I_{13/2}$) and ($^4F_{3/2}\rightarrow{}^4I_{15/2}$) respectively for glass specimens.

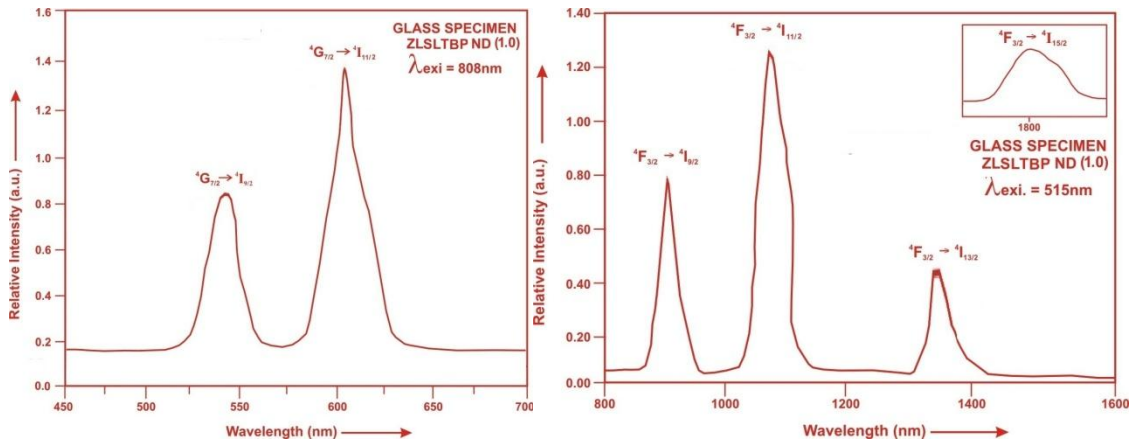

Fig.5: Fluorescence spectrum of ZLSLTBP ND(1.0) glass

The wavelengths of these bands along with their assignments are given in **Table 6**.

Table 6. Emission peak wave lengths (λ_p), radiative transition probability (A_{rad}), branching ratio (β_R), stimulated emission crosssection (σ_p), and radiative life time (τ_R) for various transitions in Nd^{3+}doped ZLSLTBP glasses.

Transition		ZLSLTBP ND (1.0)				ZLSLTBP ND (1.5)				ZLSLTBP ND (2.0)			
	λ_{max} (nm)	$A_{rad}(s^{-1})$	β	σ_p (10^{-20} cm^2)	τ_R(μs)	$A_{rad}(s^{-1})$	β	σ_p (10^{-20} cm^2)	τ_R (μs)	$A_{rad}(s^{-1})$	β	σ_p (10^{-20} cm^2)	τ_R (10^{-20} cm^2)
$^4G_{7/2}\rightarrow{}^4I_{9/2}$	532	3525.84	0.4426	0.505		3472.30	0.4484	0.522		3419.02	0.4546	0.532	
$^4G_{7/2}\rightarrow{}^4I_{11/2}$	595	2944.37	0.3696	1.091		2778.04	0.3587	1.082		2609.45	0.3470	1.071	
$^4F_{3/2}\rightarrow{}^4I_{9/2}$	905	913.16	0.1146	0.876		911.70	0.1177	0.906		910.58	0.1211	0.927	
$^4F_{3/2}\rightarrow{}^4I_{11/2}$	1075	503.93	0.0633	2.224	125.52	502.90	0.0649	2.363	129.13	502.17	0.0668	2.564	132.97
$^4F_{3/2}\rightarrow{}^4I_{13/2}$	1320	77.61	0.0097	0.431		77.41	0.0099	0.441		77.28	0.0102	0.456	
$^4F_{3/2}\rightarrow{}^4I_{15/2}$	1800	1.85	0.0002	0.026		1.85	0.0002	0.026		1.85	0.0002	0.027	

V. Conclusion

In the present study, the glass samples of composition :(30-x)P_2O_5:10ZnO:10Li_2O:10Na_2O:10CaO:10WO_3:20B_2O_3:xNd_2O_3. (where x =1, 1.5, 2 mol %) have been prepared by melt-quenching method. The stimulated emission cross section (σ_p) has highest value for the transition ($^4F_{3/2}\rightarrow{}^4I_{11/2}$) in all the glass specimens doped with Nd^{3+} ion. This shows that ($^4F_{3/2}\rightarrow{}^4I_{11/2}$) transition is most probable transition. The results show that the Nd^{3+} doped borophosphate glasses could be potential candidates for 1075 nm photonic devices. The value of (T_c-T_g) is found to be greater than 100 ^{0}C, which is a necessary condition to achieve fibre drawing.

References

[1]. Meena,S.L.(2025).Spectral and Raman Analysis of Tb^{3+} doped Yttrium Zinc Lithium Ceasium Barium Borate Glasses,IOSR Appl.Phys.17,41-47.

[2]. Yordanova,A.,Milanova,M.,Aleksandrov,L.,Iordanova,R.,Tzvetkov,P.,Markov,P.,Petrov,P.(2025).Preparation of glass-ceramic materials by controlled crystallization of Eu_2O_3 doped WO_3-B_2O_3-La_2O_3 glasses and their luminescent properties,30,832,1-12.

[3]. Kashif,I.,Ratep,A.(2022).Luminescence in Er^{3+} co-doped bismuth germinate glass-ceramics for blue and green emitting applications,60,511-526.

[4]. Meena,S.L.(2020).Spectral and Thermal properties of Eu^{3+} ions doped zinc lithium alumino antimony borogermanate glasses,Int.J.Eng.Sci.Inv.9,10-16.

[5]. Meena,S.L.(2024).Spectral and Thermal properties of Tm^{3+} doped in zinc lithium tungsten antimony borophosphate glasses,IOSR Appl.Phys.16,10-15.

[6]. Singh,H.,Singh,D.,Singh,S.P.(2025).Er^{3+},Nd^{3+},Tm^{3+}:Up-conversion in lead borophosphate glasses for visible emission,J.Fluo.35,5145-5157.

[7]. Kolobkova,E.,Grabtchikov,A.,Khodasevich,I.(2021).Upconversion luminescence and energy transfer in the flurophosphate glasses with low phosphate content doped with Tm^{3+} and Yb^{3+} ions,J.Non Cryst.Solids,11-12,100065.

[8]. Pisarska,J.,Kuwik,M.,Pisarski,W.A.(2021).Spectroscopic properties of inorganic glasses doped with Pr^{3+}: Acomparative study,Mat.15,767,1-14.

[9]. Garcia,R.N.,Desirena,H.,Luke,T.L.,Contreras,J.G.,Jayasankar,C.K.,Torres,R.Q.,Rosa,E.De la(2015).Spectroscopic properties of Eu^{3+}/Nd^{3+} co-doped phosphate glasses and opaque glass-ceramics,Opt.Mat.46,34-39.

[10]. Zhu,Y.Z.,Shen,X.,Zhou,M.,Su,X.,Li,J.,Yang,G.,Shao,H.,Zhou,Y.(2019).Ultra-broad band 1.0μm band emission spectroscopy in Pr^{3+}/Nd^{3+}/Yb^{3+} tri-doped tellurite glass,Spectrochimica Acta Part A:Mol. Biomol. Spect.222,117178.

[11]. El-Maaref,A.A.,Badr,S.,Shaaban,Kh.S.,Wahab,E.A.A.,Elokr,M.M.(2019).Optical properties and radiative rates of Nd^{3+} doped zinc-sodium phosphate glasses,J.Rare-Earths,37,253-259.

[12]. Guidini,P., Galleani.G., Faria,W., Silva,I.D.A., Eckert, H.(2020). Structural and spectroscopic properties of phosphate tungsten glasses doped with Nd^{3+} and Tb^{3+},J.Non Cryst.Solids,529,119752,1-10.

[13]. Tian,C.,Chen,Xi,Shuibao,Yu(2015).Concentration dependence of spectroscopic properties and energy transfer analysis in Nd^{3+} doped bismuth silicate glasses,Solid State Sci.48,171-176.

[14]. Meena,S.L.(2021). Spectral and Thermal properties of Pr^{3+} doped lead lithium sodium tungsten borophosphate glasses,IOSR Appl.Phys.13,1-7.

[15]. Meena,S.L.(2021). Spectral and Raman Analysis of Er^{3+} doped Zinc Lithium Antimony Sodalime Tellurite Glasses,Int.J.Eng.Sci.Inv.10,09-15.

[16]. Judd, B.R. (1962). Optical Absorption Intensities of Rare Earth Ions. Physical Review, 127, 750.

[17]. Ofelt, G.S. (1962). Intensities of Crystal Spectra of Rare Earth Ions. The J. Chem. Phys., 37, 511.

[18]. Kashif,I.Ratep,A.(2023).Luminescence in Er^{3+} co-doped bismuth germinate glass-ceramics for blue and green emitting applications,J.Korean Ceram.Soc.60,511-526.

[19]. Meena,S.L.(2021).Spectral and Raman Analysis of Sm^{3+} doped in Zinc Lithium Sodalime Alumino Silicate Glasses,Int.J.Eng.Sci.Inven.10,28-33.

[20]. Meena,S.L.(2025).Spectral,Thermal and Raman Analysis of Dy^{3+} doped Borosilicate Glasses with Large Thermal Stability Parameter,Int.J.Eng.Sci.Inv.14,11-18.

[21]. Yin,Qianwen,Kang,S.,Wang,X.,Li,S.,He,D.,Hu,L.(2017).Effect of PbO on the spectral and thermo-optical properties of Nd^{3+} doped phosphate laser glass,Opt.Mat.66,23-28.

[22]. Weber,M.J.,Myers,J.D.,Blackburn,D.H.(1981).Optical properties of Nd^{3+} in tellurite and phosphotellurite glasses,J.Appl.Phys.52,2944-2949

[23]. Lin,X.,Liang,H.,Jiang,X.,Liu,L.,Wang,Z.,Luo,Y.(2022).Thermal and fluorescence properties of Nd_2O_3-doped Gd_2O_3-Ga_2O_3-GeO_2 glass based on the Judd-Ofelt theory,J.Non-Cryst.Solids,594,121810.

[24]. Sumalatha,C.,Doddoji,R.,Venkateswarlu,M.,Rekha Rani,P., Swapna,K., Mahamuda,S.K.,Rao,A.S.(2020).White light emission from Dy^{3+} doped $ZnO+Bi_2O_3+BaF_2+B_2O_3+TeO_2$ glasses: Structural and spectroscopic properties,Spectrochim Acta A. Mol Biomol Spect.240,118568.

[25]. Lalla,E.A.,Rodriguez-Mendoza,U.R.,Lozano-Gorrin, A.D.,Sanz-Arranz,A., Rull,F., Lavin,V.(2016).Nd^{3+} doped TeO_2-PbF_2-AlF_2 glasses for laser applications,Opt.Mater,51,35-41.